IEEE Access
Multidisciplinary | Rapid Review | Open Access Journal

Received 29 December 2024, accepted 31 January 2025, date of publication 5 February 2025, date of current version 13 February 2025.

Digital Object Identifier 10.1109/ACCESS.2025.3539550

RESEARCH ARTICLE

TLEABLCNN: Brain and Alzheimer's Disease Detection Using Attention-Based Explainable Deep Learning and SMOTE Using Imbalanced Brain MRI

EROL KINA
Özalp Vocational School, Van Yüzüncü Yıl University, 65800 Van, Türkiye
e-mail: erolkina@yyu.edu.tr

ABSTRACT Alzheimer's disease (AD) is one of the primary causes of dementia. It degenerates the brain and reduces the activity of individuals by disrupting their memory and physiological functions. A comprehensive examination of specific brain tissue is required in order to accurately diagnose a brain condition using magnetic resonance imaging. The main aim of this research was to develop a rapid and effective technique for detecting healthy persons before the onset of brain tumours, including AD, pituitary tumours, gliomas, and meningiomas. This work presents a lightweight convolutional architecture based on EfficientNet with a Squeeze Attention Block using transfer learning. The proposed approach used lightweight layers with an L2 regularizer, global pooling (2D), and batch normalisation to construct the model, including two dropout layers. This paper utilises the synthetic minority oversampling approach to address the issues of overfitting and imbalanced samples by balancing two significantly imbalanced MRI datasets. We evaluated the efficacy of the minority strategy by doing experiments on both the training set and the entire dataset. The proposed model demonstrates high efficiency, with the risk of overfitting mitigated by applying SMOTE solely to the training data, while the test and validation datasets remain unaffected. The effectiveness of the proposed approach was evaluated using several performance measures and compared with previous published research. We evaluated the proposed approach for explainability via gradient-weighted class activation mapping to comprehend the model's behaviour and its predictions. The proposed framework offers advantages over existing models in terms of computing efficiency, explainability, generalization, and clinical significance.

INDEX TERMS Brain tumor, Alzheimer's disease, deep learning, machine learning, SMOTE, XAI.

I. INTRODUCTION

Alzheimer's disease (AD) is one of the most alarming neurological diseases impacting the aged worldwide. Alzheimer's disease first affects the brain areas associated with memory and cognition. In 2010, almost 600,000 people 65 and older lost their lives to Alzheimer's. The senior mortality rate dropped to 32%. As a result, authors in analysis [1] developed a well-informed estimate of the annual mortality rate among older adults with Alzheimer's disease in the United States between 2010 and 2050. A mental condition will affect 50 million individuals globally in 2022, making it the most critical concern in social and health services. Concerns over AD escalate with advancing age [2], [3]. The irreversible degeneration of neurons due to AD impairs the ability to remember recent occurrences, recognize known individuals, or identify loved ones. This results in persons being bewildered since they cannot comprehend their surroundings. AD and related dementias currently affect 6.9 million Americans who are 65 years of age or older. This figure could increase to 13.8 million by 2060 if medical advancements fail to prevent or cure AD. In 2021, Alzheimer's disease was

The associate editor coordinating the review of this manuscript and approving it for publication was R. K. Tripathy.

© 2025 The Authors. This work is licensed under a Creative Commons Attribution 4.0 License.
For more information, see https://creativecommons.org/licenses/by/4.0/

responsible for 119,399 fatalities, according to official death certificates [4], [5]. It is very important to look into the causes of neurological diseases, like Alzheimer's disease, as the world's population ages to make sure everyone is healthy. The exact way that Alzheimer's disease works is still unknown, even though the illness is very complicated. In the last few decades, experts have found many things that put people at risk for AD, such as high blood pressure, smoking, and not having enough schooling [6].

Brain tumours and AD are two significant neurological issues that greatly affect the structure and function of the brain. Brain tumours may arise when the brain or other tissues, such as the medulla or blood vessels, undergo rapid growth [7]. Despite the fact that the precise origins of these tumours are largely unknown, metabolic alterations, ovarian suppression, and ageing factors may contribute. These tumours may be either benign or malignant. AD, a degenerative disease that typically affects elderly individuals, is characterised by the accumulation of beta-amyloid plaques and tau protein deposits in the brain. Due to its unique nature, a combination of environmental, behavioural, and genetic variables influences mental health development [8]. Symptoms of cerebral palsy are contingent upon the location, intensity, and severity of the stroke. This pattern encompasses cognitive issues, seizures, headaches, and liver or kidney injury. Conversely, Alzheimer's disease begins with mild memory loss and amnesia, which progresses to severe cognitive decline, speech difficulties, and memory loss. Both frequently disrupt daily activities and place significant demands on carers, who must contend with financial, emotional, and psychological obstacles [9], [10].

MRI is a beneficial technique for the ongoing surveillance and diagnosis of Alzheimer's disease and brain tumor. In the context of brain tumours, MRI scans generate precision images that facilitate the identification of the tumour's nature, assessment of its size and severity, and support the decision-making process for treatments such as surgery or therapy. MRI is an invaluable instrument for the early detection of structural abnormalities, such as cerebral hydrocephalus, in AD. Modern imaging methods, like diffusion tensor imaging (DTI) and magnetic resonance imaging, give a lot of information about the brain's structure and changes. This is important for early diagnosis, follow-up, and treatment suggestions. They possess the capacity to generate patterns [11].

AI methods are more effective for disease detection, especially deep learning, because they capture intricate patterns and important neurons from the image data. Explainable artificial intelligence (XAI) refers to a collection of practices and methods that are designed to enhance the user friendliness and reliability of deep or learning models. The paradigm of deep learning, which stands for fairness, responsibility, and openness, is founded on two fundamental concepts: XAI and deep learning. XAI may be advantageous for organizations that are striving to increase the confidence of their AI applications. By employing XAI, they are capable of comprehending the actions of an AI model and identifying health issues. Explainable AI can facilitate and improve decision-making by offering valuable data and insights. For instance, XAI can emphasize the critical aspects of the model's predictions and direct the selection of the optimal course of action to accomplish the desired result.

A. CHALLENGES

The complex nature of the differences makes diagnosing medical conditions particularly Alzheimer's disease extremely challenging. The number of patients for the Alzheimer's disease type is often inadequate, despite the datasets size, which causes sampling bias and makes generalisation difficult. Deep learning models perform well on basic data, but their excessive power limits their ability to generalise quickly when faced with complicated situations. Because these models depend on a weight distribution for motion, they often fall short in capturing the whole spectrum of motion artefacts in medical imaging. A detailed anatomical examination of the disease, especially MRI, is necessary for an accurate diagnosis. Conventional techniques, such physical visualisation of clinical data and patient records and manual tissue extraction, are labour-intensive, time-consuming, and heavily reliant on medical personnel. Even while some research have used typical machine learning algorithms on MRI data, these approaches often result in mistakes and diagnostic blunders, making it challenging to provide precise and trustworthy diagnoses. This emphasises the need of innovative and creative approaches to raise the standard and effectiveness of therapeutic patient care.

B. CONTRIBUTIONS

Deep learning is an advanced AI technique that improves and accelerates the detection process. These techniques need a significant volume of data to correctly classify each image in biological image classification. A potential solution to this problem is to acquire knowledge from others [11]. The proposed approach autonomously extract significant information from MRI, potentially circumventing the limitations of current methodologies using the imbalanced data and accelerates training via the implementation of synthetic oversampling technique. The contributions of the study are as follows:

- This study proposes a transfer learning, EfficientNet Squeeze Attention Block-based convolutional lightweight architecture. The proposed approach utilised lightweight layers with an L2 regularizer, global pooling (2D), and batch normalisation to design the model using two dropout layers.
- To overcome the problem of overfitting and imbalanced samples, this study employs the synthetic minority oversampling technique to balance two highly imbalanced MRI datasets. We assessed the effectiveness of the minority technique by conducting experiments on both the training and the entire dataset.

- The efficacy of the proposed approach was assessed using different performance metrics and compared with other published studies.
- We checked the proposed approach to explainability using gradient-weighted class activation mapping to understand the model's behaviour and its predictions.

The rest of the paper is structured like: Brain tumor classification and Alzheimer's disease related research are under Section II. Section III analyses the procedure and evaluates the proposed approach, including topics such as data preparation, dataset splitting, and sampling technique. Section IV presents the results and discussion, while Section V presents the conclusion.

II. LITERATURE

Numerous factors contribute to dementia, with AD being one of the most prevalent. As the disease advances from mild to severe, doing everyday activities independently becomes more difficult. It was shown in a study [12] that a Gated Recurrent Unit and a Vision Transformer can be used to reliably and accurately find signs of AD in MRI images. Upon capturing a photograph, the ViT enables the GRU to form specific connections among the pertinent components of the image. The suggested model efficiently and precisely addresses the class mismatch problem in the MRI image dataset, surpassing state-of-the-art methods. The VGG16 deep learning model is renowned for its efficacy in image recognition tasks; researchers are now exploring its use for extracting detailed information from MRI and PET images. Their objective in using deep learning was to discern nuanced patterns suggestive of Alzheimer's disease [13]. The authors intended to convey a substantial quantity of quality across the network by using the idea of a thick block. To maintain the relative significance of each attribute, min-max pooling layers were used. The authors transitioned to Inception-block for all convolutional layers to reduce the number of parameters while increasing their variability. Through PCA, they successfully reduced the characteristics to just the most significant ones [14]. The authors created a CNN design that can quickly find brain tumours in MRI. Using contrasts with ResNet-50, VGG16, and Inception V3 helps to check the suggested design. To find out how well a model worked, they looked at its accuracy, recall, loss, and AUC. Based on these tests, the suggested model did better than others. The CNN model did well on 3264 MR images, with a recall of 91.19%, an accuracy of 93.3%, an area under the curve of 98.43%, and a loss of 0.25 [15]. Separate research presented a strategy for autonomous lesion detection in MRI scans using residual neural networks. Trial results on the BRATS dataset demonstrate the effectiveness of the suggested neural network [16].

The main aim of work [17] was to examine and assess two different methods for AD detection, along with five separate deep learning models. When employees choose not to provide new data, they revert to the CNN design. The work [18] employed quantum machine learning classifiers as part of an ensemble deep learning model in their proposal to classify Alzheimer's disease. Combining the datasets from the Alzheimer's Disease Neuroimaging Initiative I and II results in the classification of Alzheimer's disease. Using changed versions of the VGG16 and ResNet50 models, they put people into four groups based on how mild, moderate, or very mild their dementia was. These groups were no dementia, mild dementia, and moderate dementia. The research [19] endeavours to classify AD through MRI in order to facilitate swift interventions and optimal therapy. Training used 80% of the dataset, while validation and testing used 10%. The VGG16 design aims to achieve an accuracy of 87%. So, generative adversarial networks (GANs) were used in study [20] to add to the data and improve classification results while reducing overfitting. Mujahid et al. [21] research presented a distinctive framework that enhances the interpretability of the suggested system for brain tumour diagnosis via the use of explainable AI approaches. They integrated support vector machines with the optimised recursive feature elimination method to enhance interpretability. The proposed method enhances detection task performance by eliminating superfluous characteristics and emphasising the most critical ones.

CNN, in particular, employed a deep learning methodology in paper [22]. The proposed approach employed transfer learning via the importation of pre-trained models for medical image categorisation, including EfficientNetB7. During the development process, it was common practice to perpetually extend CNN at an increasing cost in order to achieve greater accuracy as resources increase. The pre-trained EfficientNetB7 model used a compound coefficient in its CNN architecture and scaling strategy to make the sizes of the inputs the same. The recommended EfficientNetB7 model demonstrated superior efficiency, simplicity, and speed when compared to VGG19 and InceptionV3. The proposed model is unique because it has simple building blocks and low computational complexity. The objective of paper [23] was to investigate the development of a deep learning infrastructure that can accurately identify and classify the stages of Alzheimer's disease. The proposed analytical method used 2D T1-weighted MR brain images and CNN architecture. The proposed approach [24] focused on employing CNNs to identify objects in MRI images, particularly AD and brain tumor. It has always been challenging to choose the ideal settings, requiring either extensive trial-and-error or specialised expertise. For CNNs to succeed, this procedure is crucial. The authors developed a hybrid approach to address this issue, using the PSO algorithm to determine the optimal CNN design configuration. They intended to reduce the loss function value and increase the Area Under Curve (AUC) scores for illness forecasting by using the PSO algorithm.

The research [25] suggested transfer learning in a deep ensemble model, in order to identify AD patients in a collection of many instances. To make the very uneven Alzheimer's disease dataset's classes more equal, the authors

TABLE 1. Comparative analysis of strength and weaknesses.

Study	Strengths	Weaknesses
[12]	Introduces an innovative method for precise AD classification utilizing a ViT-GRU model and explainable artificial intelligence approaches. The method achieved superior outcomes for three-class datasets.	The proposed methodology exclusively classified data pertaining to Alzheimer's disease; brain tumors were not addressed in that research.
[13]	The research identified profound features and utilized machine learning for Alzheimer's disease classification.	The authors conducted trials with restricted data and obtained suboptimal results with the machine learning models.
[14]	The research employed a random forest model and attained superior outcomes. The advantage lies in the utilization of PCA for feature extraction.	The study did not utilize brain imaging to identify brain tumors and instead on binary classification. The multi-class issue is overlooked.
[15]	To reduce the fatality rate and improve accuracy, the study classified brain tumors using MRI images.	The model employs numerous layers, potentially escalating costs, and its conclusions are not elucidated through XAI.
[17]	The positive aspect is that the authors improved the accuracy of the data and outcomes by using deep learning both with and without augmentation. The authors have also developed hybrid learning.	The model has many layers, which could lead to more costs, and model cannot explain its findings.
[19]	The inception model uses a lightweight network and performs exceptionally well, making predictions based on features. The study employed edge detection, gray scaling preprocessing, and accuracy improvement.	The primary deficiency is the absence of XAI models that improve trust and elucidate the model's decisions.
[21]	The study used supervised learning with hybrid features, preprocessing, augmentation, and feature selection. The study used feature eliminating to achieve outclass performance.	Important features that are vulnerable may be eliminated by the feature selection technique. Additionally, the investigation exclusively concentrates on brain tumors.
[23]	High performance, improved AD diagnosis, local and global classification, and comparison analysis were all achieved by the study.	The study did not generalize well, had problems with overfitting, had limited model explainability, and did not use all available criteria to improve the dataset.
[24]	The study employed hyper-parameter optimization and the image preprocessing CLAHE approach and augmentation to strengthen the model's performance and employ validation statistics.	Due to its limited generality and reliance on ADNI data, the complex model requires more time to train and analyze.

used adaptive synthetic oversampling. In identifying disease instances, the proposed model has a 97.35% accuracy rate. Compared to the DenseNet-121 and Xception models employed alone, the DenseNet-121+Xception ensemble model had an 18% higher accuracy. In order to train and evaluate the proposed model, authors obtained the MRI scan dataset from the ADNI database [26].

To prepare the raw data for processing, the authors used the CLAHE image enhancement technique. By adding new data, they were able to correct the dataset's irregularities, resulting in 60,000 image data points distributed among six groups. Five models—VGG16, MobileNetV2, AlexNet, ResNet50, and InceptionV3—received test scores of 78.84%, 86.85%, 78.87%, 80.98%, and 96.31%, respectively, according to their initial training and testing. Vaiyapuri et al. [27] developed a brain tumour classification ensemble learning-driven Driven Computer-Aided Diagnosis Model (ELCAD-BTC) using MRIs. The system's description states that its objective is to identify and classify various BT processes. This method uses gabor filtering to reduce noise and enhance the clarity of MRI images. Additionally, they utilized ensemble learning to extract features using three deep learning models: MobileNet, DenseNet, and EfficientNet. Also, the researchers developed a unified TumorDetNet DL model [28] that is capable of automatically identifying and categorising brain tumours. The model based on deep learning can correctly identify brain tumours and divide them into three types: meningioma, pituitary, and meningioma; as well as two other types: dangerous and normal. The proposed approach is different from the state-of-the-art work due to its compatibility, various training data, computation and explainability of model. Also, it achieved outclass results with transfer learning. Other studies did not utilize sampling techniques completely or apply them before splitting, which caused overfitting and the same samples in the test data. The comparative analysis of strength and weaknesses is shown in Table 1.

III. MATERIALS AND METHODS

This section comprises a dataset description, preprocessing, data splitting, sampling techniques, and the proposed methodology. Figure 1, and a detailed explanation is provided in subsections.

A. DATASET DESCRIPTION

This study utilized publicly available Kaggle datasets related to Alzheimer's and brain diseases, and integrated them for multiclass classification into seven classes. This study randomly selects some samples from the dataset. After collecting and merging the data, we preprocess it by reshaping it into fixed-size input for deep learning models. The dataset is divided into three sets: train, test, and validation, with 70:20:10 ratios. We reshape the data again and encode the labels. Following that, the proposed TLEABLCNN model is developed and trained using training data. The obtained dataset is very imbalanced and has a limited sample size, thus we must balance it at this point. For this, the oversampling synthetic minority approach is used on both the full dataset and only the training data. The effectiveness of the oversampling strategy is evaluated for balanced training and the entire data. Then the trained model is evaluated on test and validation data to check its performance. The model makes accurate detections of brain and AD cases.

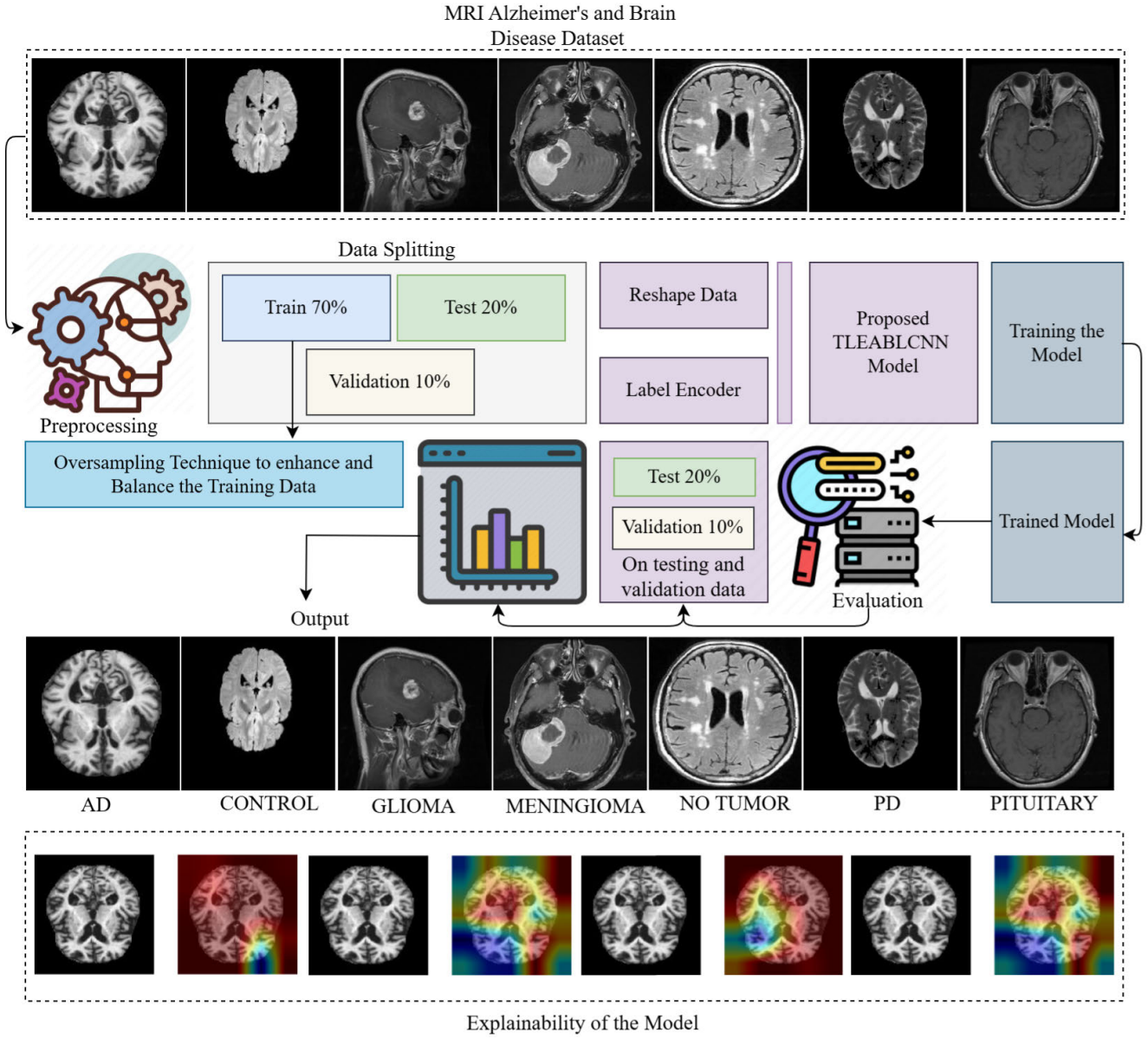

FIGURE 1. The workflow of the proposed study incorporates MRI brain and AD datasets, preprocessing, data splitting, oversampling techniques, and the methodology.

Also, the proposed model is validated with explainability using the Grade-CAM method. The workflow of the proposed methodology is shown in

B. PREPROCESSING

Image processing refers to the study of digital photography and the use of computer algorithms to manipulate and understand them. Image processing aims to improve the visual quality of a image, extract useful information from it, and prepare it for experiments or interpretation. When it comes to computer vision and image processing, few methods are as popular or as powerful as OpenCV. Altering the size of a image is as simple as using scaling procedures. We need to convert the collected photographs into a fixed-size input file for deep learning as they arrive in different formats. One more thing: normalisation is just putting all of the pixel intensities in a image within a predetermined range. In 8-bit depth images, this range is typically 0-255, with 255 representing white and 0 representing black. When processing or improving contrast, it is helpful to standardise the pixel values [29].

C. SYNTHETIC MINORITY OVERSAMPLING TECHNIQUE

The Synthetic Minority Over-sampling Technique (SMOTE) creates artificial samples for the minority class to fix the issue of class imbalance, which has an effect on how well deep learning models work. Majority classes have a strong place, while minority classes are not well represented. SMOTE makes examples of minority classes to fix this problem and get a fair spread of classes. In the feature space of the

TABLE 2. Before and after applying SMOTE, the number of samples of each class.

Diseases	Label	Imbalanced Samp	Balanced Samp
AD	0	3200	3650
CONTROL	1	3650	3650
PD	2	906	3650
NO TUMOR	3	405	3650
MENINGIOMA	4	306	3650
PITUITARY	5	300	3650
GLIOMA	6	300	3650

minority class, SMOTE creates synthetic cases. When one or more classes are significantly under-represented compared to others, MOTE works with information to fix the problem. The first step is to find the minority class or groups in the information. SMOTE finds the k instances of the minority class that are closest to each other in the feature space [30]. The number of close neighbour, shown by the letter k, is the user-defined option. For each case of a minority class, SMOTE picks one of its k close neighbours at random. After that, synthetic samples are made along the line section that goes from the minority class instance to the chosen closest neighbour in the feature space. It makes synthetic cases to help the minority class better understand important trends and decision lines. It prevents overfitting when models do well on training data but poorly on data they haven't seen before in datasets that aren't fair. Furthermore, SMOTE makes it easier to make a model that works for everyone by producing extra data [31]. Before and after applying SMOTE, the number of samples of each class is illustrated in Table 2.

D. DATASET SPLITTING

The process of dividing data into two or more classes is referred to as data splitting. Researchers often use one segment of a bifurcated dataset for model training and the remaining segment for evaluation or testing. A vital element of data science is data partitioning, especially when using data to develop models. Researchers use the training data set to develop and train models. Upon completion of training, they use the testing dataset [32]. To verify the appropriate functionality of the final model, we conduct a comparison between the training and test datasets. The data set was divided into three sets in a 70:20:10 ratio: training, testing, and validation. Splitting of imbalance MRI dataset into 70:20:10 is shown in Table 3. Data splitting into 70:20:10, applied oversampling on Full MRI dataset is shown in Table 4, and oversampling only training data is shown in Table 5.

E. METHODOLOGY

We design the transfer learning Efficient attention block lightweight convolution network using deep learning framework renowned for its exceptional performance and computational efficiency balance. Utilising pre-trained weights from ImageNet, the model offers a strong basis for sharing features gleaned from large and varied datasets. In addition to

TABLE 3. Splitting of imbalance MRI dataset into 70:20:10.

Diseases	Train data	Test data	Validation data
AD	2240	640	320
CONTROL	2550	730	365
PD	633	182	91
NO TUMOR	284	81	40
MENINGIOMA	214	61	31
PITUITARY	210	60	30
GLIOMA	210	60	30
Total	6346	1814	907

TABLE 4. Data splitting into 70:20:10, applied oversampling on Full MRI dataset.

Diseases	Train data	Test data	Validation data
AD	2555	730	365
CONTROL	2555	730	365
PD	2555	730	365
NO TUMOR	2555	730	365
MENINGIOMA	2555	730	365
PITUITARY	2555	730	365
GLIOMA	2555	730	365
Total	17885	5110	2555

TABLE 5. Data splitting into 70:20:10, applied oversampling only training data.

Diseases	Train data	Test data	Validation data
AD	2555	640	320
CONTROL	2555	730	365
PD	2555	182	91
NO TUMOR	2555	81	40
MENINGIOMA	2555	61	31
PITUITARY	2555	60	30
GLIOMA	2555	60	30
Total	17885	1814	907

supporting 150×150×3 RGB input images, it enables us to develop unique input layers for our particular requirements by eliminating the top classification layer (include_top=False). To fit the model to our data, we eliminated everything except the last 20 features and then design the novel approach. The attention mechanism, which enhances the model's capacity to classify the most crucial elements of an impact, is one of its primary features. Initially, this technique shrinks the feature map to a fraction of the global edge representation. Proposed lightweight architecture is represented in Figure 2.

The first squeeze global pooling layer decreases the vector's dimension based on the sampling rate, while the second layer uses a sigma implementation to estimate the vector's initial size and determine the prediction weight. These prediction weights then boost important features and suppress less significant ones on the feature map. This focus technique improves the model's performance and interpretability by helping it retain important aspects of the data, particularly in crucial tasks like feature extraction. After the prediction block, the model adds a thin convolution layer to get more spatial information from the data and keep it from fitting too well. The Conv2D layer with 32 filters and 3 × 3 vectors makes up the feature map that was extracted using

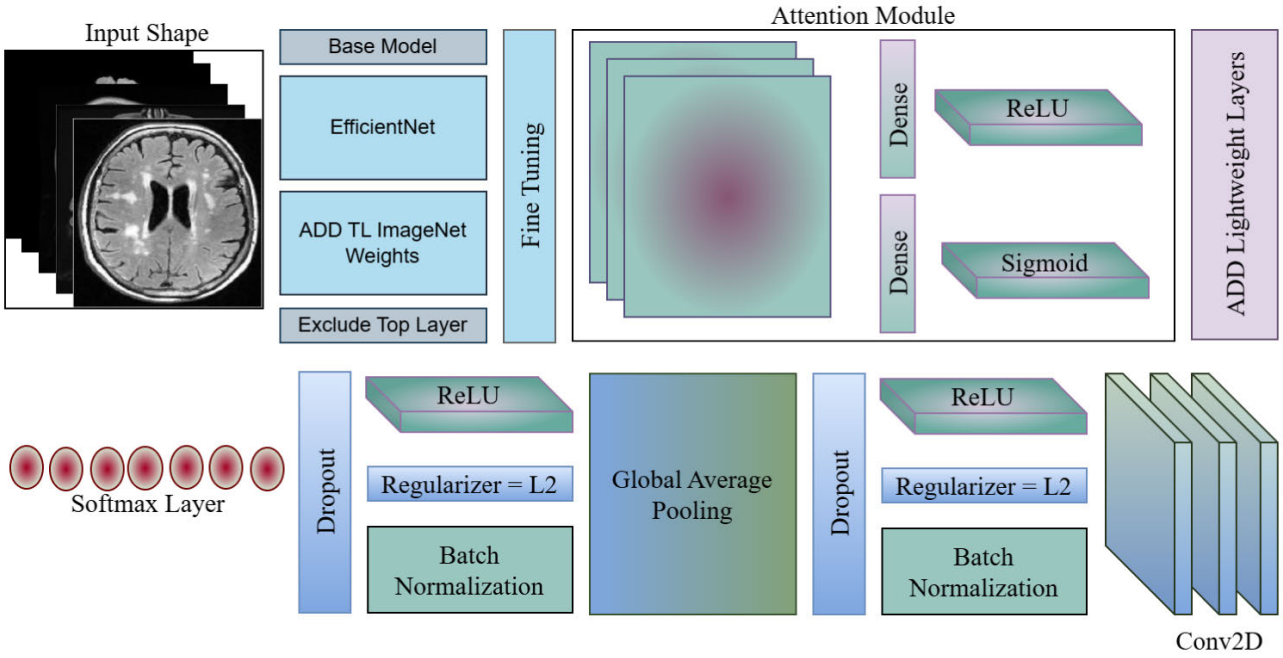

FIGURE 2. Proposed transfer learning, EfficientNet Squeeze Attention Block-based convolutional lightweight architecture.

the emphasis approach. We use a ReLU implementation to visualise it nonlinearly.

The addition of block normalisation, which expedites training but is less sensitive to particular features, allowed the model to be trained more effectively and handle various subsets of the data. We used a 20% dropout threshold to enhance the model's generalisation ability by preventing incorrect classification of certain neurones during training. These convolutional layers act as a link between the prediction algorithm and the last classification layer. They make sure that the model creates useful features without fitting them too well. After all, the model goes from extracting features to classifying them. The global average pooling layer combines the features into a vector so that the 256 neurones can pick up on the complex correlations in the data and send the activation. L2 normalisation minimises outliers, while output normalisation guides training. Additionally, the second dropout ratio of 40% lowers the likelihood of cross-correlation. With seven neurones, the output layer is appropriate for task involving multiclass detetion. We use Adam analysis, known to increase the learning rate with experience during training, to optimise the model. It is shown that accuracy and AUC can be used to judge how well a model works, and a cross-validation loss function is used to rule out misclassification based on model accuracy. These design components work together to provide a reliable and effective model for challenging classification tasks.

The primary advantage of the ReLU function over other activation functions is that it does not activate every neurone simultaneously. Batch normalisation extends normalisation beyond the input layer of a neural network to include all hidden layers as well. Batch normalisation mitigates the effects of internal covariate shift on the network's convergence during training by standardising the activations across all layers. Although L2 regularisation considerably decreases the weights, it neither yields a sparse solution nor renders them zero.The regularisation parameter l2 penalises all parameters except the intercept, therefore ensuring the model generalises the data and mitigates overfitting.

IV. RESULTS AND DISCUSSION

This section provides the experimental results of the proposed model, using imbalanced and balanced training data, cross-validation experiments and comparisons with other state-of-the-art pretrained models. Also, different performance metrics are utilised for the efficacy of the model. Accuracy is one of the most straightforward methods for assessing the performance of a classification model. It ultimately comes down to the number of precise predictions that the model accurately generates. The rate of accomplishment for optimistic forecasts is one definition of precision. The percentage of true positives that are correctly identified is known as recall, which is frequently abbreviated as sensitivity. It is the ratio of genuine positive results to the total of both true positives and false negatives. The F1-Score is obtained by harmonically aggregating recall and accuracy. In order to achieve equilibrium between the two issues, it is possible to consolidate the two metrics into a singular value. One method of evaluating the performance of a classification model across all thresholds is to examine

its Receiver Operating Characteristic (ROC) curve. AUC is a statistical measure that denotes the area under the ROC curve. AUC-ROC provides a comprehensive evaluation of a classifier's performance by considering all prospective thresholds [33].

$$\text{Accuracy} = \frac{\text{TPP} + \text{TNP}}{\text{TPP} + \text{FNP} + \text{FPP} + \text{TNP}} \quad (1)$$

$$\text{Precision} = \frac{\text{TPP}}{\text{TPP} + \text{FPP}} \quad (2)$$

$$\text{Recall} = \frac{\text{TPP}}{\text{TPP} + \text{FNP}} \quad (3)$$

$$\text{F1 score} = 2 \times \frac{\text{Precision} \times \text{Recall}}{\text{Precision} + \text{Recall}} \quad (4)$$

The experiments are conducted using an Intel Core i7 10th generation processor operating at 2.60 GHz, accompanied by 16GB of RAM, running Windows 11. The Anaconda Jupyter Notebook is used to do experiments using TensorFlow libraries on a 13.9GB NVIDIA GPU. The proposed approach used 70% of the data for training and the remainder for evaluation. The experimental design employs categorical cross-entropy loss, a learning rate of 0.0001 for the Adam optimizer, 15 epochs, and a batch size of 64.

A. INVESTIGATION OF RESULTS FOR IMBALANCE MRI DATA

Table 6 presents the results for Imbalance MRI using the testing data. The proposed model achieved 0.8239 precision for AD, 94.74 for CONTROL, 0.80 for PD, 0.7719 for No TUMOUR, 0.9524 for MENINGIOMA, and 0.8364 for PITUITARY brain tumor. The model also achieved 0.9547 recall for AD and 0.80 for glioma brain tumor. Also, it achieved a 0.8958 F1 score for AD disease.

Table 7 displays the results of Imbalance MRI using the validation data. The proposed model achieved 0.8864 precision for AD, 0.9379 for CONTROL, 0.9630 for PD, 0.80 for No TUMOUR, 0.8837 for MENINGIOMA, and 0.9070 for PITUITARY brain umor. The model also achieved 0.9750 recall for AD and 0.9667 for glioma brain tumor. Also, it achieved a 0.9286 F1 score for AD disease.

TABLE 6. Results for imbalance MRI using testing data.

Disease	Label	Precision	Recall	F1 score
AD	0	0.8239	0.9547	0.8958
CONTROL	1	0.9474	0.7973	0.8661
PD	2	0.8000	0.9333	0.8615
NO TUMOR	3	0.7719	0.7213	0.7458
MENINGIOMA	4	0.9524	0.9877	0.9697
PITUITARY	5	0.8364	0.9835	0.9040
GLIOMA	6	0.9412	0.8000	0.8649

Figure 3 displays the confusion matrix findings of the proposed approach, which uses imbalanced data. The label 0 shows 312 accurate outcomes out of 320; the label 1 shows 317 accurate outcomes; the label 2 shows 26 accurate and 4 inaccurate outcomes. Label 4 has only two inaccurate outcomes; it achieved outclass performance. Additionally, Label 6 did exhibit one error in its classification.

TABLE 7. Results for imbalance MRI using validation data.

Disease	Label	Precision	Recall	F1 score
AD	0	0.8864	0.9750	0.9286
CONTROL	1	0.9379	0.8685	0.9018
PD	2	0.9630	0.8667	0.9123
NO TUMOR	3	0.8000	0.7742	0.7869
MENINGIOMA	4	0.8837	0.9500	0.9157
PITUITARY	5	0.9070	0.8571	0.8814
GLIOMA	6	0.9355	0.9667	0.9508

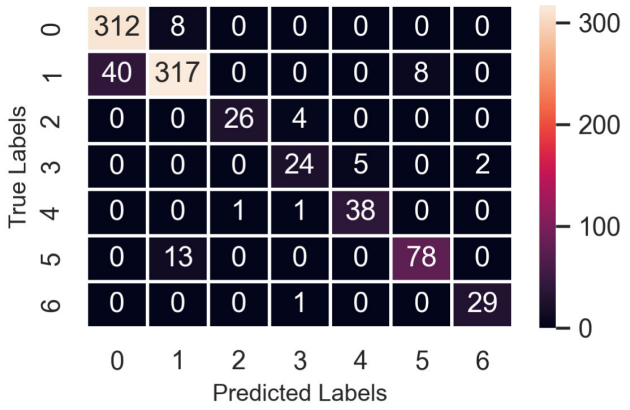

FIGURE 3. Confusion matrix findings of the proposed approach using imbalance data.

True positives and false positive rates of the proposed approach for ROC-AUC are displayed in Figure 4. Label 3 achieved minimum AUC of 0..9690 and label 4 achieved 0.9997 AUC. The curves shows the performance of the proposed approach for multi-class classification with AUC. The precision and Recall curves of the proposed approach, showed average precision for multi-class classification is presented in Figure 5.

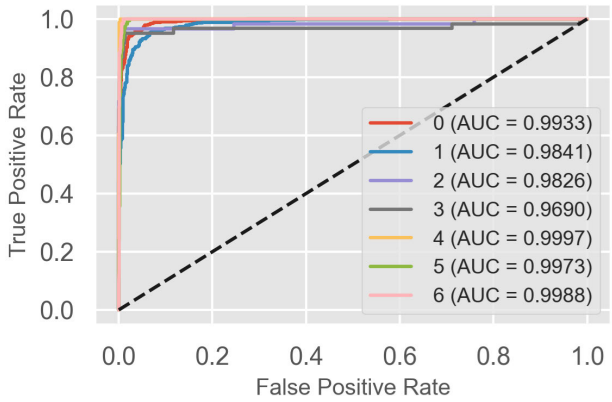

FIGURE 4. True positives and false positive rates od the proposed approach for ROC-AUC.

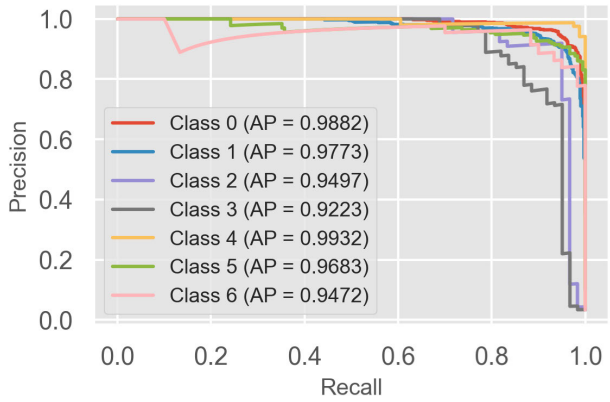

FIGURE 5. The precision and Recall curves of the proposed approach, showed average precision for multi-class classification.

B. INVESTIGATION OF RESULTS FOR BALANCED MRI DATA

Table 8 displays the balance MRI results based on test data. The precision of the suggested model was 0.9368 for AD, 0.8508 for CONTROL, 0.8644 for PD, 0.8197 for NO TUMOUR, 0.9639 for MENINGIOMA, and 0.8636 for PITUITARY brain tumour. Additionally, the model's recall for AD was 0.8344, and for glioma brain tumours, it was 0.90. Additionally, its F1 score for AD illness was 0.8826.

Table 9 displays the balance MRI results utilising validation data. The precision of the suggested model was 0.9217 for AD, 0.9322 for CONTROL, 0.9310 for PD, 0.8333 for No TUMOUR, 0.9268 for MENINGIOMA, and 0.90 for PITUITARY brain tumour. Additionally, the model's recall for AD was 0.9563, and for glioma brain tumours, it was 0.9667. Additionally, its F1 score for AD illness was 0.9387.

TABLE 8. Results for balance MRI using testing Data.

Disease	Label	Precision	Recall	F1 score
AD	0	0.9368	0.8344	0.8826
CONTROL	1	0.8508	0.9137	0.8811
PD	2	0.8644	0.8500	0.8571
NO TUMOR	3	0.8197	0.8197	0.8197
MENINGIOMA	4	0.9639	0.9877	0.9756
PITUITARY	5	0.8636	0.9396	0.9000
GLIOMA	6	0.9153	0.9000	0.9076

TABLE 9. Results for balance MRI using validation data.

Disease	Label	Precision	Recall	F1 score
AD	0	0.9217	0.9563	0.9387
CONTROL	1	0.9322	0.9041	0.9179
PD	2	0.9310	0.9000	0.9153
NO TUMOR	3	0.8333	0.8065	0.8197
MENINGIOMA	4	0.9268	0.9500	0.9383
PITUITARY	5	0.9000	0.8901	0.8950
GLIOMA	6	0.9355	0.9667	0.9508

Figure 6 illustrates the confusion matrix results of the proposed approach, which merely used oversampling to the training data. The testing and validation aspects of the method continue to be imbalanced. Out of 320 possible outcomes, the label 0 displays 306 accurate outcomes, the label 1 displays 330 accurate outcomes, and the label 2 displays 27 accurate outcomes and three wrong results. In addition to achieving outstanding performance, Label 4 has two results that are not accurate. Moreover, Label 6 did have one mistake in its classification, which was quite unfortunate.

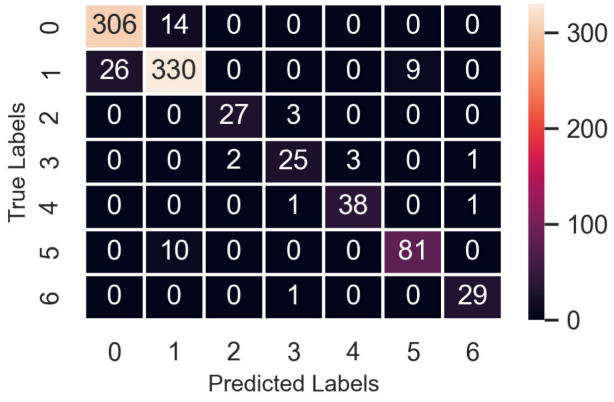

FIGURE 6. Confusion matrix findings of the proposed approach applied oversampling only for training data, testing and validation remains imbalanced.

Figure 7 shows the true positive and false positive rates for the proposed ROC-AUC method. Label 4 had an AUC of 0.9998, whereas Label 3 obtained a minimum AUC of 0.9785. For the proposed approach, label 0 obtained an AUC of 0.9945, whereas label 5 had an AUC of 0.9956. The graphs illustrate how well the recommended approach performs in multi-class classification using AUC. Figure 8 displays the precision and recall curves of the proposed approach, which demonstrated average precision for multi-class categorisation.

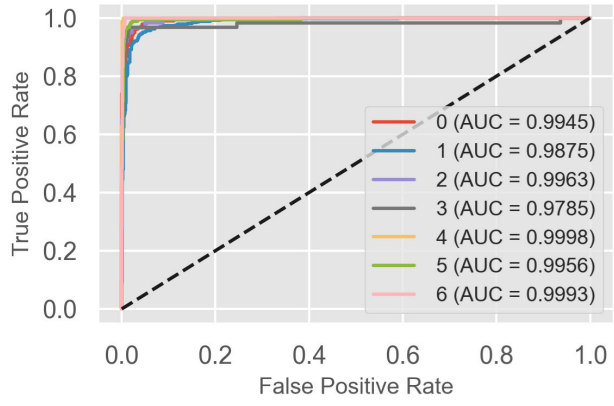

FIGURE 7. True positives and false positive rates od the proposed approach for ROC-AUC.

C. INVESTIGATION OF RESULTS FOR BALANCED MRI ENTIRE DATA

Table 10 presents the findings of the balancing MRI by making use of the test data. A total of 0.9307 for Alzheimer's disease, 0.8184 for control, 0.9752 for Parkinson's disease, 0.9693 for no tumour, 0.9905 for meningioma, and 0.9739 for

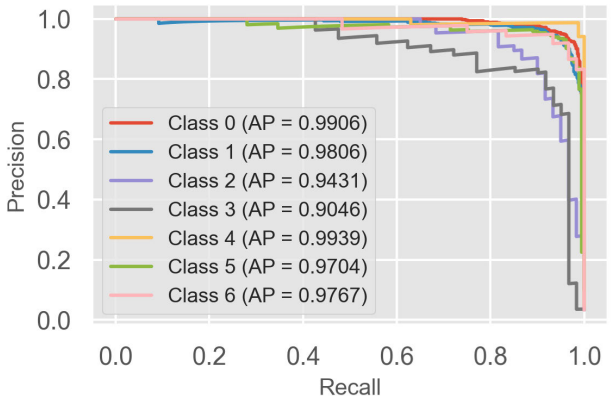

FIGURE 8. The precision and Recall curves of the proposed approach, showed average precision for multi-class classification.

pituitary brain tumour were the accuracy values that the suggested model attained. For glioma brain tumours, the model obtained a recall of 0.9890, while for Alzheimer's disease, it achieved a recall of 0.9307. Additionally, it was able to get a score of 0.98100 on the F1 diagnostic scale for glioma.

Table 11 presents the outcomes of the MRI balancing, which are based on the validation data. The accuracy of Alzheimer's disease was 0.8291, the accuracy of the control was 0.9654, the accuracy of Parkinson's disease was 0.9702, the accuracy of no tumour was 0.9857, the accuracy of meningioma was 0.9946, and the accuracy of pituitary brain tumour was 0.9678. According to the glioma brain lesions, the model was able to acquire a recall of 1.00 and an AD of 0.9836. Another glioma brain tumour had an F1 score of 0.9878, which was likewise the case.

TABLE 10. Results for balance MRI using testing Data.

Disease	Label	Precision	Recall	F1 score
AD	0	0.9307	0.8274	0.8760
CONTROL	1	0.8184	0.9137	0.8634
PD	2	0.9752	0.9712	0.9732
NO TUMOR	3	0.9693	0.9507	0.9599
MENINGIOMA	4	0.9905	0.9959	0.9932
PITUITARY	5	0.9739	0.9699	0.9719
GLIOMA	6	0.9730	0.9890	0.9810

TABLE 11. Results for balance MRI using validation data.

Disease	Label	Precision	Recall	F1 score
AD	0	0.8291	0.9836	0.8997
CONTROL	1	0.9654	0.7644	0.8532
PD	2	0.9702	0.9808	0.9755
NO TUMOR	3	0.9857	0.9452	0.9650
MENINGIOMA	4	0.9946	1.0000	0.9973
PITUITARY	5	0.9678	0.9890	0.9783
GLIOMA	6	0.9759	1.0000	0.9878

Figure 9 displays the confusion matrix findings of the proposed approach, which applied oversampling on entire data. The label 0 shows 359 accurate outcomes out of 365; the label 1 shows 279 accurate outcomes; the label 2 shows 358 accurate and 7 inaccurate outcomes. Label 4 has no inaccurate outcomes; it achieved outclass performance. Additionally, Label 6 did not exhibit any errors in its classification.

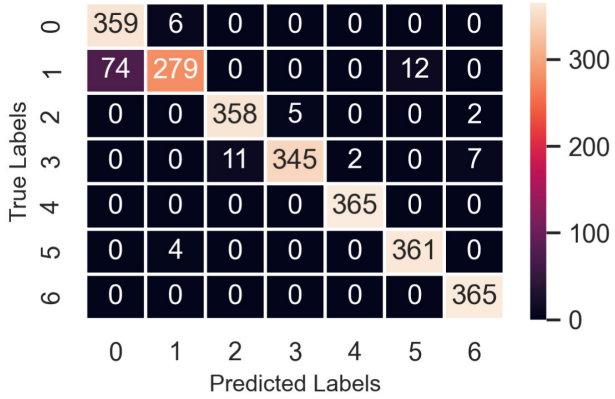

FIGURE 9. Confusion matrix findings of the proposed approach applied oversampling on entire data.

Figure 10 illustrates the true positive and false positive rates for the proposed ROC-AUC method. Label 4 demonstrated an AUC of 0.9999, while Label 0 achieved a minimum AUC of 0.9980. Label 2 achieved an AUC of 0.9960 for the proposed approach, while label 5 achieved an AUC of 0.9996. Label 3 obtained an AUC of 0.9984. The graphs demonstrate the effectiveness of the recommended approach in multi-class classification when employing AUC. Figure 11 illustrates the precision and recall contours of the proposed approach, which exhibited an average precision for multi-class categorisation.

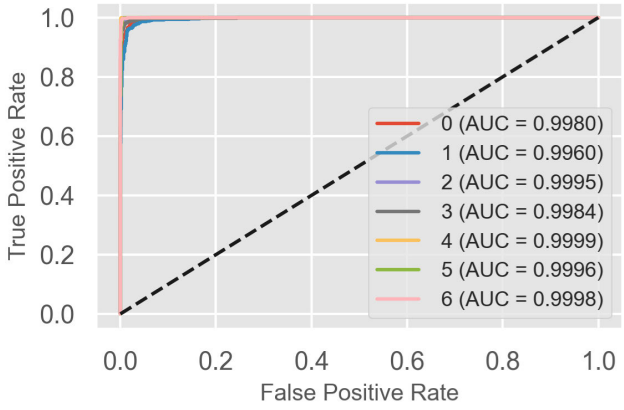

FIGURE 10. True positives and false positive rates od the proposed approach for ROC-AUC.

D. COMPARATIVE ANALYSIS OF PERFORMANCE FOR THE PROPOSED APPROACH

Comparative analysis of performance for the proposed approach in perspective of imbalanced and balanced data is shown in Figure 12. In the first, we did experiments using imbalanced data to check the efficacy of the proposed

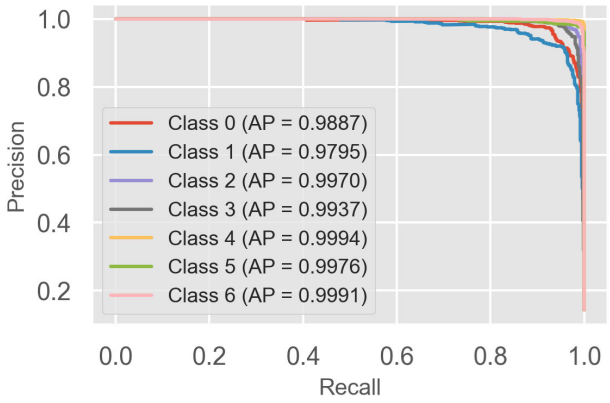

FIGURE 11. The precision and Recall curves of the proposed approach, showed average precision for multi-class classification.

approach, and then we applied the SMOTE technique on only training data to balance the imbalanced dataset in the 2nd experiment. For the third experiment, we applied the technique to the entire data set. Using imbalanced data, we got 90.85% validation accuracy; using only balanced training data, we got 92.17%, and lastly, after applying the SMOTE technique on the entire data, we got 95.19% validation accuracy. We can see that there is little improvement using the SMOTE technique only on training data, but validation data remains imbalanced. In addition, when we applied SMOTE on the entire (training and validation) set, we got a 4.34% improvement in results.

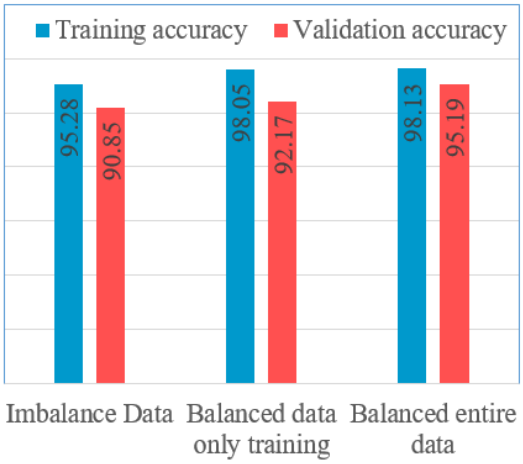

FIGURE 12. Comparative analysis of performance for the proposed approach in perspective of imbalance and balanced data.

E. LEARNING CURVES AND AUC

Learning curves serve as a prevalent diagnostic technique for models in machine or deep learning that progressively acquire knowledge from a dataset. Curves of the measured performance may be generated, and the model can be evaluated on the training, testing and holdout validation datasets after each training update. This enables the visualization of learning curves. Learning curves are graphical representations that illustrate the variation in an individual's learning performance as their experience increases. The accuracy curve, serves as a measure of the model's performance in generating predictions based on the data, tracking its progress during the training, testing and validation process as shwon in Figure 13, 14, and 15. The loss curve indicates the discrepancy between the model's anticipated and actual outputs, hence offering insight into the model's performance as shown in 13, 14, and 15. The discrepancy illustrates the extent to which the actual values diverge from the model's predictions. With each successive training iteration, the model's performance consistently improves. As time advances, the loss curve illustrates the variation in the model's loss values. Despite the initial substantial loss, it diminishes as the model's performance improves. The loss, defined as the disparity between expected and actual output, signifies that a reduced value reflects enhanced accuracy in the model's predictions. A decrease in loss signifies enhanced efficacy.

Table 12 shows the complexity analysis of the proposed model using three modified datasets. Imbalance has 196 seconds of time; balance-only training takes 464 seconds, and the entire balanced dataset has 525 seconds.

TABLE 12. Complexity analysis of the proposed model.

Datasets	Computational time
Imbalance	196 Sec
Balance (only training)	464 Sec
Balance (entire data)	525 Sec

F. COMPARATIVE ANALYSIS OF PERFORMANCE OF THE PROPOSED APPROACH WITH PREVIOUS STUDIES

A comparative study of the proposed approach's performance against previously investigated methods is conducted and shown in Table 13. The investigators in the study [14] used conv2d blocks to send a lot of quality over the network. Min-max pooling layers maintained attribute importance. The authors switched to Inception-block for all convolutional layers to minimise parameters and increase variability. PCA reduced attributes to their most important ones. The authors in another study [15] developed a CNN to swiftly detect brain tumours in MRI. Comparing the proposed design to ResNet-50, VGG16, and Inception V3 helps. They evaluated models based on accuracy, recall, loss, and AUC. The recommended model performed better in these tests. The CNN model performed well on 3264 MR images, achieving 91.19% recall, 93.31% accuracy, 98.43% AUC, and 0.25% loss. In another study, residual neural networks were used to identify MRI lesions autonomously. Results from the BRATS dataset show the efficacy of the proposed neural network [16]. Sangeetha et al. [19] employed MRI data and achieved 86.87% accuracy using VGG16 model. Goyal et al. [20] utilized MRI 3 class data, with ensemble of AlexNet and LSTM model for only 200 images. The image samples was very less and achieved 96.83% accuracy and caused overfitting with less data. Our methodology surpassed other networks in performance, as seen by Table 13. The proposed

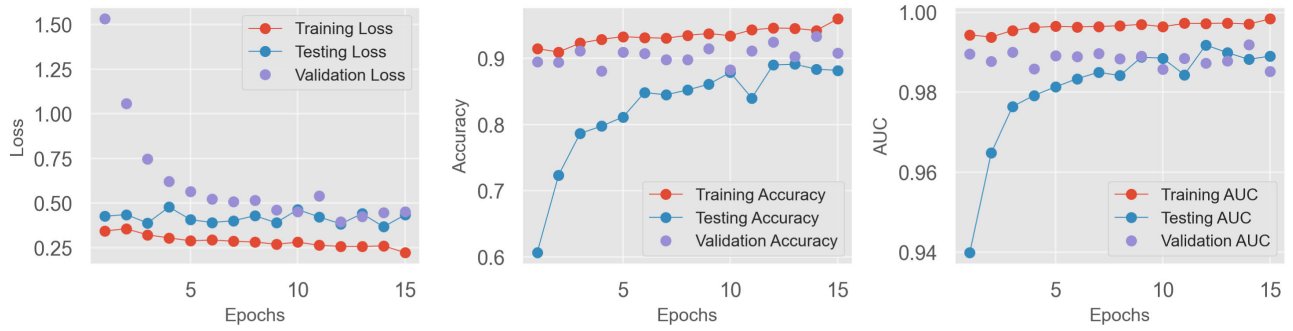

FIGURE 13. Learning curves and AUC of the proposed approach using imbalanced data: the right-side graph presents the AUC, the left side presents the loss, and the middle graph presents the accuracy.

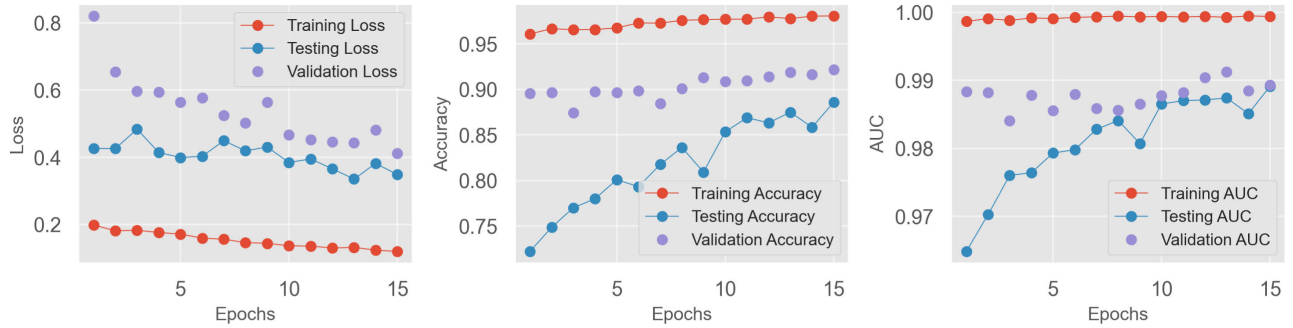

FIGURE 14. Learning curves and AUC of the proposed approach using balanced data (applied oversampling only on training data): the right-side graph presents the AUC, the left side presents the loss, and the middle graph presents the accuracy.

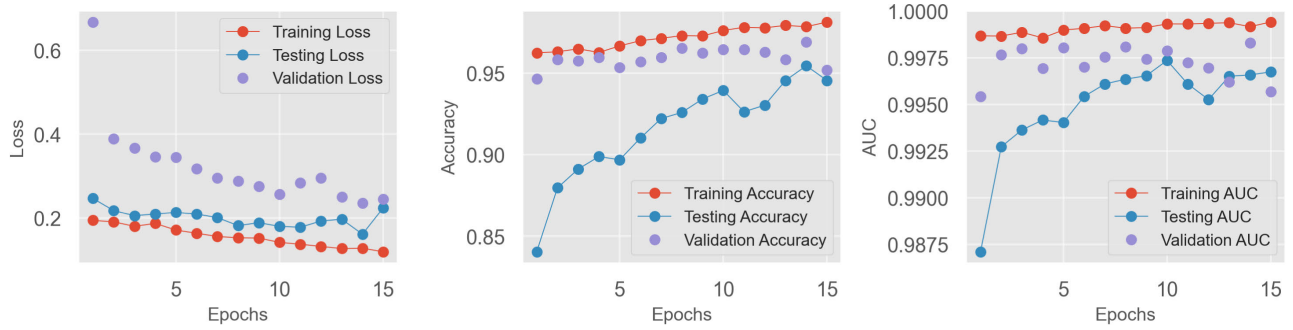

FIGURE 15. Learning curves and AUC of the proposed approach using balanced data (applied oversampling on entire data): the right-side graph presents the AUC, the left side presents the loss, and the middle graph presents the accuracy.

model surpassed existing models, achieving an overall accuracy rate of 95.19% in the proposed technique.

G. GRAD-CAM USING PROPOSED MODEL

We can analyse and understand the results produced by the proposed approach using Gradient-weighted Class Activation Mapping in deep learning as represented in Figure 16.

This strategy converts them from ambiguous models into clear narratives by uncovering the concealed choices made by the proposed approach. Grad-CAM identifies the essential feature maps for each class by analysing the gradients in the final convolutional layer. Understanding the significance of interpretability will facilitate the comprehension and explanation of network-based models. Master the principles of Grad-CAM visualisation to analyse and understand model selections. Acquire knowledge on using Grad-CAM, a technique that generates class activation maps to emphasise the segments of MRI that are pivotal for model predictions.

The proposed model's capacity to execute deep learning models with high confidence and accuracy—particularly in the diagnosis of brain tumors—is significantly impacted by the Grad-CAM results. It gives crucial information and aids in demonstrating the model's predictions by explicitly identifying the brain images that the AI is targeting for the doctors. This aids in bridging the gap between practitioner expertise and AI effects. As a result, it is essential for early cancer diagnosis and therapy, which improves patient outcomes and protection.

TABLE 13. Comparative analysis of performance of the proposed approach with previous studies.

Author	Data	Classes	Model	Images	Accuracy	Year
Hazarik et al. [14]	MRI	2	RF	-	98.08	2023
Hassan et al. [13]	MRI	5	SVM	2640	93.84	2024
Mahmud et al. [15]	MRI	4	CNN	3264	93.31	2023
M. Reza Obeidavi and K. Maghooli [16]	MRI	2	CNN	2200	94.43	2022
Sangeetha et al. [19]	MRI	4	VGG16	6400	86.87	2024
Goyal et al. [20]	MRI	3	AlexNet+LSTM	200	96.83	2024
This work	MRI	7	TLEABLCNN	20606	95.19	2024

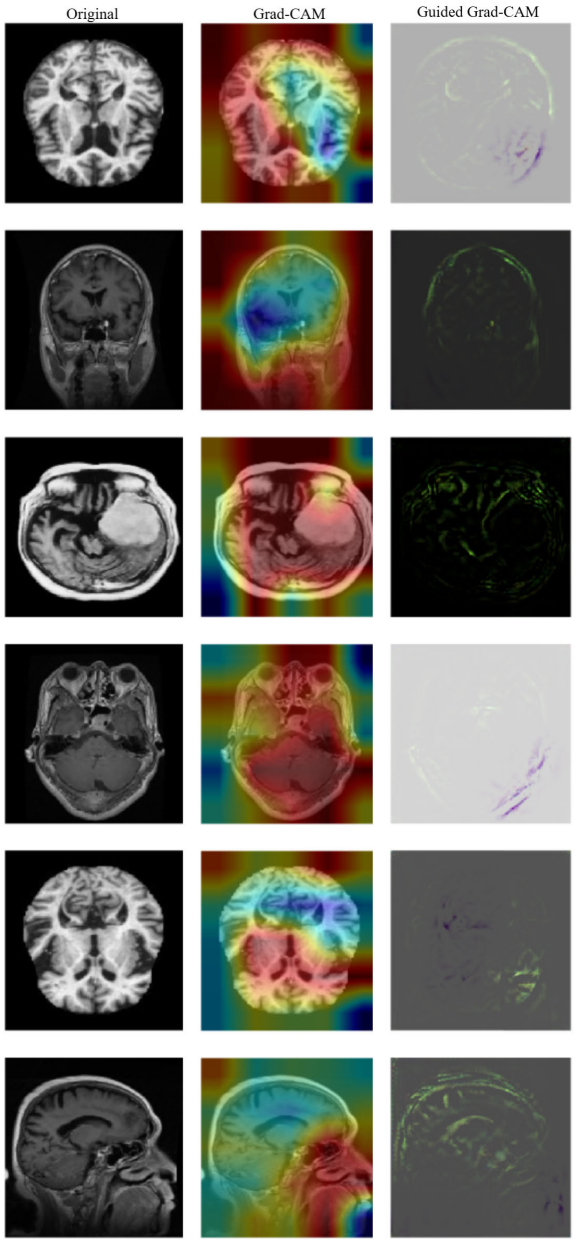

FIGURE 16. GCAM- Visualization.

This approach may enhance the accuracy and ease of brain tumor diagnosis for radiologists, thereby minimizing diagnostic errors and facilitating expedited treatment. When incorporated into clinical workflows, it could serve as a helpful supportive model, particularly in resource-constrained hospitals. This entails evaluating the model on more large and heterogeneous data sets, integrating several imaging modalities such as MRI and CT, or employing advance localization techniques as Grad-CAM to enhance the robustness and comparability of the results.

V. CONCLUSION

The use of multiclass datasets presents difficulties in the rapid diagnosis and classification of neurological disorders such as Alzheimer's. An accurate automated method is required for diagnosing and treating the condition. This study introduced a lightweight and efficient convolutional architecture that employs EfficientNet Squeeze Attention Blocks and transfer learning. The model was constructed using two dropout layers to identify occurrences of Alzheimer's disease from a multiclass dataset. It used lightweight layers including an L2 regularizer, global 2D pooling, and batch normalisation. Due of the significant imbalance in the Alzheimer disease dataset, we used a SMOTE sampling method to equilibrate the classes.

The experimental findings indicated that the proposed approach attained training accuracies of 95.28%, 98.05%, and 98.13%, as well as validation accuracies of 90.85%, 92.17%, and 95.19% for imbalanced, balanced training data, and entirely balanced data, respectively. The proposed approach attained a maximum AUC of 99.93, a minimum AUC of 97.85, a best average precision of 99.39, and a lowest average precision of 90.46. The GLIOMA brain tumor incurred just a single error in the classification task. Overall, the sampling technique enhances the performance of the proposed model. The proposed designs are suitable, as they are fundamental structures that offer controllable timing with reduced computational complexity, memory requirements, and overfitting, as indicated by the experiments' results.

The proposed framework demonstrates deficiencies in certain scenarios, such as control and non-tumor cases, where it attained subpar performance across all metrics. In the future, we will concentrate on weak cases through the application of feature extraction and selection techniques.

CONFLICTS OF INTEREST

"The author declare no conflict of interest."

REFERENCES

[1] J. Weuve, L. E. Hebert, P. A. Scherr, and D. A. Evans, "Deaths in the United States among persons with Alzheimer's disease (2010–2050)," *Alzheimer's Dementia*, vol. 10, no. 2, pp. e40–e46, Mar. 2014, doi: 10.1016/j.jalz.2014.01.004.

[2] A. B. Q. Steiner, A. F. Jacinto, V. F. D. S. Mayoral, S. M. D. Brucki, and V. D. A. Citero, "Mild cognitive impairment and progression to dementia of Alzheimer's disease," *Revista da Associação Médica Brasileira*, vol. 63, no. 7, pp. 651–655, Jul. 2017, doi: 10.1590/1806-9282.63.07.651.

[3] M. Khojaste-Sarakhsi, S. S. Haghighi, S. M. T. F. Ghomi, and E. Marchiori, "Deep learning for Alzheimer's disease diagnosis: A survey," *Artif. Intell. Med.*, vol. 130, Aug. 2022, Art. no. 102332.

[4] *World Alzheimer Report 2018*, Alzheimer's Disease Int., State Art Dementia Research: New Frontiers; Alzheimer's Disease Int. (ADI), London, U.K., 2018, pp. 14–20.

[5] Alzheimer's Association, "2024 Alzheimer's disease facts and figures," Alzheimer's & Dementia, Chicago, IL, USA, pp. 3708–3821, 2024, vol. 20, doi: 10.1002/alz.13809.

[6] M. A. Better, "Alzheimer's disease facts and figures," *Alzheimers Dement*, vol. 19, no. 4, pp. 1598–1695, 2023.

[7] M. Pichaivel, G. Anbumani, P. Theivendren, and M. Gopal, "An overview of brain tumor," *Brain Tumors*, vol. 1, pp. 1–10, Jan. 2022.

[8] B. Borroni, C. Costanzi, and A. Padovani, "Genetic susceptibility to behavioural and psychological symptoms in Alzheimer disease," *Current Alzheimer Res.*, vol. 7, no. 2, pp. 158–164, 2010.

[9] F. Ghandour, A. Squassina, R. Karaky, M. Diab-Assaf, P. Fadda, and C. Pisanu, "Presenting psychiatric and neurological symptoms and signs of brain tumors before diagnosis: A systematic review," *Brain Sci.*, vol. 11, no. 3, p. 301, Feb. 2021.

[10] J. Jiménez-Balado and T. S. Eich, "GABAergic dysfunction, neural network hyperactivity and memory impairments in human aging and Alzheimer's disease," *Seminars Cell Develop. Biol.*, vol. 116, pp. 146–159, Aug. 2021.

[11] A. S. Lundervold and A. Lundervold, "An overview of deep learning in medical imaging focusing on MRI," *Zeitschrift für Medizinische Physik*, vol. 29, no. 2, pp. 102–127, May 2019.

[12] S. M. Mahim, M. S. Ali, M. O. Hasan, A. A. N. Nafi, A. Sadat, S. A. Hasan, B. Shareef, M. M. Ahsan, M. K. Islam, M. S. Miah, and M.-B. Niu, "Unlocking the potential of XAI for improved Alzheimer's disease detection and classification using a ViT-GRU model," *IEEE Access*, vol. 12, pp. 8390–8412, 2024, doi: 10.1109/ACCESS.2024.3351809.

[13] A. Hassan, A. Imran, A. U. Yasin, M. A. Waqas, and R. Fazal, "A multimodal approach for Alzheimer's disease detection and classification using deep learning," *J. Comput. Biomed. Inform.*, vol. 6, no. 2, pp. 441–450, 2024.

[14] R. A. Hazarika, D. Kandar, and A. K. Maji, "A novel machine learning based technique for classification of early-stage Alzheimer's disease using brain images," *Multimedia Tools Appl.*, vol. 83, no. 8, pp. 24277–24299, Aug. 2023, doi: 10.1007/s11042-023-16379-6.

[15] M. I. Mahmud, M. Mamun, and A. Abdelgawad, "A deep analysis of brain tumor detection from MR images using deep learning networks," *Algorithms*, vol. 16, no. 4, p. 176, Mar. 2023, doi: 10.3390/a16040176.

[16] M. R. Obeidavi and K. Maghooli, "Tumor detection in brain MRI using residual convolutional neural networks," in *Proc. Int. Conf. Mach. Vis. Image Process. (MVIP)*, Ahvaz, Iran, Feb. 2022, pp. 1–5, doi: 10.1109/MVIP53647.2022.9738767.

[17] S. E. Sorour, A. A. A. El-Mageed, K. M. Albarrak, A. K. Alnaim, A. A. Wafa, and E. El-Shafeiy, "Classification of Alzheimer's disease using MRI data based on deep learning techniques," *J. King Saud Univ.-Comput. Inf. Sci.*, vol. 36, no. 2, Feb. 2024, Art. no. 101940, doi: 10.1016/j.jksuci.2024.101940.

[18] A. Jenber Belay, Y. M. Walle, and M. B. Haile, "Deep ensemble learning and quantum machine learning approach for Alzheimer's disease detection," *Sci. Rep.*, vol. 14, no. 1, p. 14196, Jun. 2024, doi: 10.1038/s41598-024-61452-1.

[19] M. Sangeetha, H. Gunasekaran, T. Azalini, J. Nakshathra, P. U. Mageshwari, and R. M. Devi, "Alzheimer's disease diagnosis and categorization using deep learning," in *Proc. Int. Conf. Cogn. Robot. Intell. Syst. (ICC-ROBINS)*, Coimbatore, India, Apr. 2024, pp. 189–199, doi: 10.1109/ICC-ROBINS60238.2024.10533928.

[20] P. Goyal, R. Rani, and K. Singh, "A multilayered framework for diagnosis and classification of Alzheimer's disease using transfer learned alexnet and LSTM," *Neural Comput. Appl.*, vol. 36, no. 7, pp. 3777–3801, Mar. 2024, doi: 10.1007/s00521-023-09301-6.

[21] M. Mujahid, A. Rehman, F. S. Alamri, S. Alotaibi, and T. Saba, "Brain tumor detection through novel feature selection using deep efficientNet-CNN-based features with supervised learning and data augmentation," *Phys. Scripta*, vol. 99, no. 7, Jul. 2024, Art. no. 075002.

[22] S. Suchitra, L. Krishnasamy, and R. J. Poovaraghan, "A deep learning-based early Alzheimer's disease detection using magnetic resonance images," *Multimedia Tools Appl.*, Jun. 2024, doi: 10.1007/s11042-024-19677-9.

[23] M. El-Geneedy, H. E.-D. Moustafa, F. Khalifa, H. Khater, and E. AbdElhalim, "An MRI-based deep learning approach for accurate detection of Alzheimer's disease," *Alexandria Eng. J.*, vol. 63, pp. 211–221, Jan. 2023, doi: 10.1016/j.aej.2022.07.062.

[24] R. Ibrahim, R. Ghnemat, and Q. A. Al-Haija, "Improving Alzheimer's disease and brain tumor detection using deep learning with particle swarm optimization," *AI*, vol. 4, no. 3, pp. 551–573, Jul. 2023, doi: 10.3390/ai4030030.

[25] M. Mujahid, A. Rehman, T. Alam, F. S. Alamri, S. M. Fati, and T. Saba, "An efficient ensemble approach for Alzheimer's disease detection using an adaptive synthetic technique and deep learning," *Diagnostics*, vol. 13, no. 15, p. 2489, Jul. 2023, doi: 10.3390/diagnostics13152489.

[26] F. M. J. M. Shamrat, S. Akter, S. Azam, A. Karim, P. Ghosh, Z. Tasnim, K. M. Hasib, F. De Boer, and K. Ahmed, "AlzheimerNet: An effective deep learning based proposition for Alzheimer's disease stages classification from functional brain changes in magnetic resonance images," *IEEE Access*, vol. 11, pp. 16376–16395, 2023, doi: 10.1109/ACCESS.2023.3244952.

[27] T. Vaiyapuri, J. Mahalingam, S. Ahmad, H. A. M. Abdeljaber, E. Yang, and S.-Y. Jeong, "Ensemble learning driven computer-aided diagnosis model for brain tumor classification on magnetic resonance imaging," *IEEE Access*, vol. 11, pp. 91398–91406, 2023, doi: 10.1109/ACCESS.2023.3306961.

[28] N. Ullah, A. Javed, A. Alhazmi, S. M. Hasnain, A. Tahir, and R. Ashraf, "TumorDetNet: A unified deep learning model for brain tumor detection and classification," *PLoS ONE*, vol. 18, no. 9, Sep. 2023, Art. no. e0291200, doi: 10.1371/journal.pone.0291200.

[29] J. Albright, "Forecasting the progression of Alzheimer's disease using neural networks and a novel preprocessing algorithm," *Alzheimer's Dementia, Translational Res. Clin. Interventions*, vol. 5, no. 1, pp. 483–491, Jan. 2019.

[30] M. Likhita, K. M. Kumar, N. S. Sasank, and M. Abhinaya, "AD-ResNet50: An ensemble deep transfer learning and SMOTE model for classification of Alzheimer's disease," in *Proc. Int. Conf. Innov. Comput. Commun.* Singapore: Springer, Feb. 2023, pp. 699–713.

[31] U. Rashmi and B. M. Beena, "Multiple machine learning models for Alzheimer's disease detection for mixed data with explainable AI," in *Proc. 15th Int. Conf. Comput. Commun. Netw. Technol. (ICCCNT)*, Jun. 2024, pp. 1–8.

[32] B. Vrigazova, "The proportion for splitting data into training and test set for the bootstrap in classification problems," *Bus. Syst. Res. J.*, vol. 12, no. 1, pp. 228–242, May 2021.

[33] J.-G. Gaudreault, P. Branco, and J. Gama, "An analysis of performance metrics for imbalanced classification," in *Proc. 24th Int. Conf. Discovery Sci.*, in Lecture Notes in Computer Science, vol. 12986, C. Soares and L. Torgo, Eds., Cham, Switzerland: Springer, Jan. 2021, pp. 67–77, doi: 10.1007/978-3-030-88942-5_6.

EROL KINA received the degree from the Faculty of Engineering and Architecture, Department of Computer Engineering, Çankaya University, in 2005, the master's degree from the Department of Physiology, Faculty of Medicine, Van Yüzüncü Yıl University, in 2015, and the Ph.D. degree from the Department of Statistics, in 2022. He completed his military service in Bayburt, in 2006. From 2006 to 2008, he worked as a Systems Engineer in private companies. He started working as a Lecturer at Özalp Vocational School, Van Yüzüncü Yıl University, in 2008, where he is currently working as an Academician.